

MESSENGER GUIDANCE AND CONTROL SYSTEM PERFORMANCE DURING INITIAL OPERATIONS

Robin M. Vaughan[†], Daniel J. O'Shaughnessy[†], Hongxing S. Shapiro[†], Gabe D. Rogers[†], Brian L. Kantsiper[†], David R. Haley[†], and Jason C. Bunn[†]

ABSTRACT

Flight operations are finally underway for the MESSENGER – Mercury Surface, Space ENvironment, GEOchemistry, and Ranging – mission. As part of NASA's Discovery program, the spacecraft will observe Mercury during flybys in 2008 and 2009 and from orbit for one Earth-year beginning in March of 2011. The guidance and control system combines extensive flight software with various sensors and actuators to maintain a 3-axis stabilized spacecraft and to implement desired velocity changes. The spacecraft was successfully launched on August 3, 2004, immediately putting the guidance and control system to the test. Initial mission events described in this paper are detumble after separation from the launch vehicle, attitude control for the initial Sun-relative rotation and in the later 3-axis inertial attitude mode, and the first trajectory correction maneuvers.

INTRODUCTION

The MESSENGER (MErcury Surface, Space ENvironment, GEOchemsitry, and Ranging) spacecraft was successfully launched from Kennedy Space Center in Florida on August 3, 2004. As part of NASA's Discovery program, MESSENGER will be the first spacecraft to closely observe the planet Mercury since the Mariner 10 flybys of the mid-1970s. MESSENGER will make one Earth flyby, two flybys of Venus, and three of Mercury prior to orbiting the planet for one Earth-year beginning in March 2011. The planetary flybys are interspersed with five large deterministic deep space maneuvers (DSMs) that target the spacecraft for its Mercury orbit insertion (MOI) maneuver in 2011. The Mercury flybys will assist in developing the focused science gathering of the year-long orbit phase of the mission.¹

Figure 1 shows the MESSENGER spacecraft configuration and the locations of some of the main engineering components and science instruments. The primary factors driving the spacecraft design were the high temperatures and radiation doses to be encountered at Mercury.² Protection from this environment is accomplished with a large sunshade, which shields the spacecraft components from direct exposure to the Sun. This shade must be kept between the main body and the Sun at all times when the spacecraft is within 0.85 AU of the Sun. The shade has been sized to allow small deviations from direct Sun pointing when needed for science observations or engineering activities. Power generation is handled with solar panels mounted on small booms that extend beyond the sunshade and are capable of rotating to track the Sun.

[†] Space Department, Mission Design, Guidance and Control Group, The Johns Hopkins University Applied Physics Laboratory (APL), Laurel, Maryland.

These are supplemented with a battery to provide power during eclipse periods when in orbit about Mercury. The spacecraft carries high-, medium-, and low-gain antenna sets for X-band communication with Earth. Two electronically steerable high-gain phased-array antennas are mounted on the sunshade and on the back of the spacecraft. Two medium-gain fanbeam antennas are co-located with the phased arrays. Each of these antenna sets nominally provides coverage in diametrically opposite quadrants of the plane normal to the sunshade; full 360° coverage in this plane is accomplished by rotating the spacecraft to follow the changing Sun and Earth positions. Four hemispherical low-gain antennas are mounted on the spacecraft to provide coverage in all directions. MESSENGER has a sophisticated propulsion system featuring both bi-propellant and mono-propellant thrusters that can operate in either blow-down or pressurized modes. This system is described in more detail in a later section.

MESSENGER carries a diverse suite of miniaturized science instruments to globally characterize the planet.³ Four of the science instruments are co-boresighted and mounted inside the launch vehicle adapter ring: two imaging cameras (Mercury Dual Imaging System – MDIS), a laser altimeter (Mercury Laser Altimeter – MLA), UV and IR spectrometers (Mercury Atmosphere and Surface Composition Spectrometer - MASCS), and an X-ray spectrometer (XRS). The two cameras are mounted on a pivot platform that extends their observing range for flybys and in orbit. Other instruments located outside the adapter ring are a gamma-ray and neutron spectrometer (GRNS), an energetic particle and plasma spectrometer (EPPS), and a magnetometer (MAG). The antennas are also used for radio science.

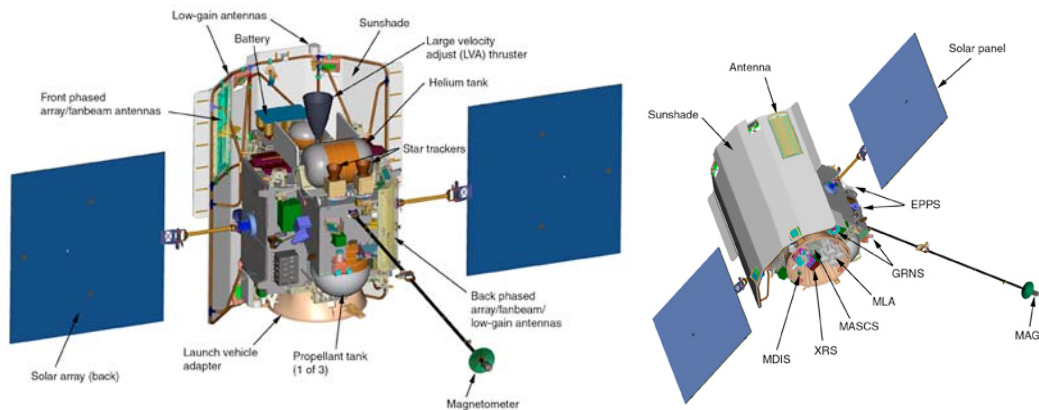


Figure 1. MESSENGER Spacecraft Components and Science Instruments

This paper begins with an overview of the guidance and control (G&C) system for MESSENGER, including the hardware components, software implementation, and functional organization. System primary functions are coordinated through the interaction of spacecraft operational modes and G&C activities performed in each mode. The remaining sections cover in-flight operations to date relating to attitude and trajectory control. System performance is illustrated by representative flight events for most primary functions. These include detumble after separation from the launch vehicle, attitude changes for G&C system tests and for other engineering and science activities, and the first three trajectory correction maneuvers (TCMs). Problems have been encountered with attitude and ΔV estimation due to a drift between the flight computer clock and the IMU's internal clock; proposed software changes to eliminate these problems are briefly described.

GUIDANCE AND CONTROL (G&C) SYSTEM OVERVIEW

The primary functions of the MESSENGER guidance and control subsystem are to maintain spacecraft attitude and to execute propulsive maneuvers for spacecraft trajectory control. Software

algorithms run in the main processor (MP) to coordinate data processing and commanding of sensors and actuators to maintain a 3-axis stabilized spacecraft and to implement desired velocity changes. The software also controls the orientation of the two solar panels, electronic steering for the two high-gain phased-array antennas, and, optionally, pivot positioning for the MDIS cameras. An additional interface with the MLA provides range and slant angle to the planet's surface used to configure the instrument but does not involve any active mechanical or electronic steering.

Any discussion of the G&C system necessarily makes extensive use of coordinate system conventions. For reference in the remaining sections, Figure 2 shows the MESSENGER spacecraft body-frame axes and the azimuth and elevation angle conventions used by the G&C system.

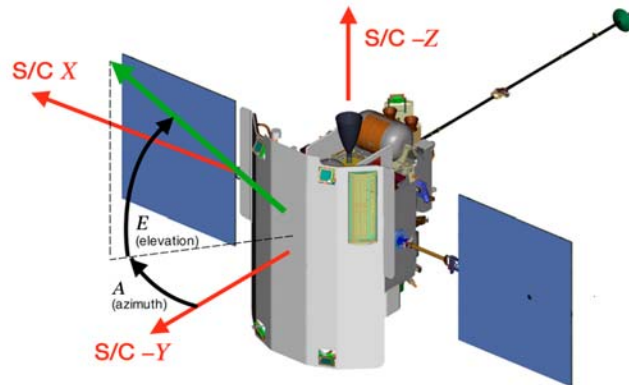


Figure 2. MESSENGER Spacecraft Coordinate System

Sensors and Actuators

The sensor suite consists of star trackers, an inertial measurement unit, and Sun sensors as shown in Figure 3. Inertial attitude reference is provided by two ASTR star trackers from Galileo Avionica, both of which are mounted on the top deck looking out along the $-Z$ axis. Typically only a single tracker is powered, with the other acting as a cold spare. Spacecraft rotation rates and translational accelerations are provided by a Northrop-Grumman S-SIRU (Scalable Space Inertial Reference Unit) inertial measurement unit (IMU) with four hemispherical resonance gyroscopes (HRGs) and Honeywell QA3000 accelerometers. The IMU has two power supply and processor boards providing internal redundancy with the second board acting as a cold spare. One board and all four gyros are powered at all times, while the four accelerometers are powered only when performing a TCM. MESSENGER also carries a set of Adcole digital Sun sensors (DSSs) to provide Sun-relative attitude knowledge if there is a failure in the primary attitude sensors. There are two separate Sun sensor systems consisting of an electronics box (DSSE) connected to three sensor heads (DSSHs), two of which are located on opposite corners of the sunshade and one on the back of the spacecraft. The Sun sensors are always powered, providing two independent Sun direction readings at all times.

The actuator suite consists of reaction wheels and thrusters as shown in Figure 4. The primary actuators for maintaining attitude control are four Teldix RSI 7-75/601 reaction wheels. All four wheels are always operating; each can provide a maximum torque of 0.075 Nm with maximum momentum storage of 7.5 Nms. Thrusters in the Aerojet propulsion system are used for attitude control during TCMs and momentum dumps and may also be used as a backup system for attitude control in the event of multiple wheel failures. The propulsion system has a large bi-propellant engine and two sets of mono-propellant thrusters - twelve 4-N thrusters and four 22-N thrusters. Eight of the 4-N thrusters, designated A1-4 and B1-4, are used for attitude control. The remaining four 4-N thrusters, designated S1&2 and P1&2, are used for small velocity changes, while the four 22-N thrusters, designated C1-4, are used for larger velocity

changes. The LVA (large velocity adjust) main engine is used for very large velocity changes, such as the five DSMs and MOI. Fuel is carried in two of the three main tanks and in the smaller auxiliary tank; the third main tank contains oxidizer for the LVA burns. A small helium tank regulates pressures of the main tanks, while the auxiliary tank is unregulated. A set of nine latch valves controls helium, fuel, and oxidizer flow between the tanks and to the thrusters. Catalyst bed heaters are provided for the 4-N and 22-N thrusters, and a flange heater is used for the LVA.

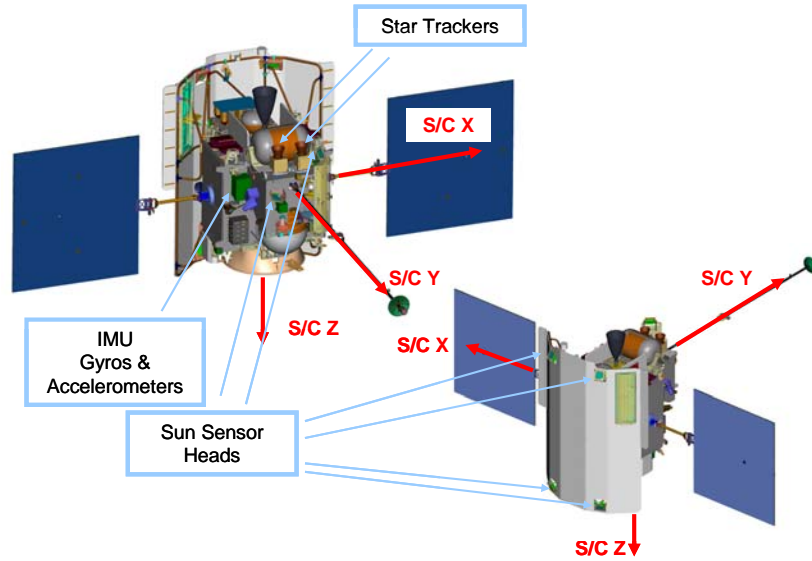


Figure 3. MESSENGER G&C Sensors

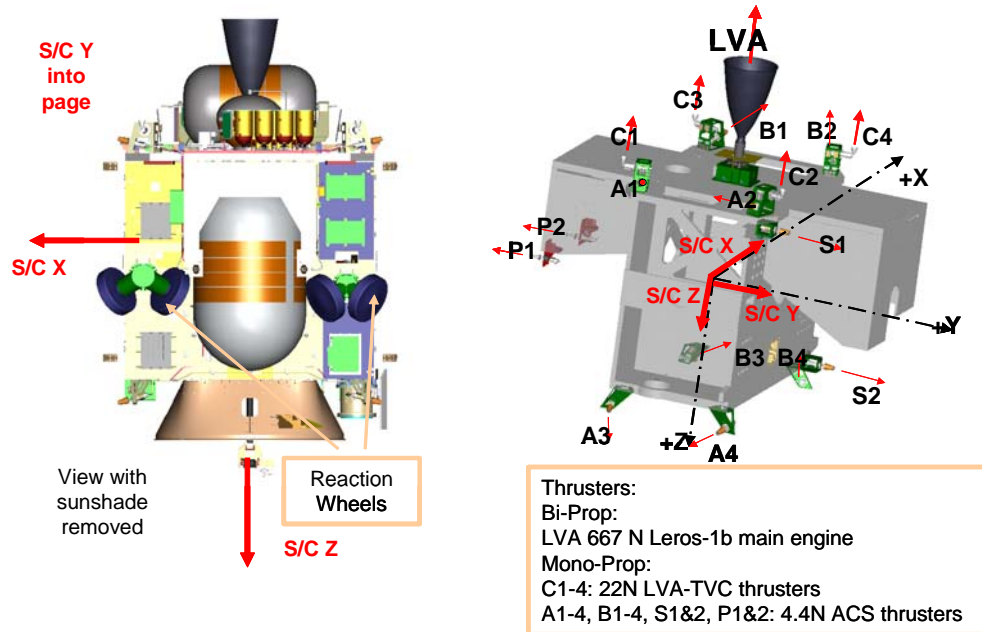


Figure 4. MESSENGER G&C Actuators

The G&C system also interfaces with actuators for three other spacecraft components. Solar panel rotation is performed using two MOOG solar array drive assemblies (SADAs). The drives can rotate in two directions about the X axis through an angular arc of 228° in the YZ plane centered at the -Z axis. Panels are rotated in steps of 0.02° at a constant rotation rate of 2°/s (100 steps per second). The beam width (or field-of-view) of the two phased-array antennas is 12° in the XY plane and 3° normal to it. The boresight, centered in this beam, can be steered through an angular arc of 120°. The antennas are mounted with boresights centered in the +X, +Y and -X, -Y quadrants. 360° coverage of Earth direction in the XY plane is obtained by rotating the spacecraft about the Y axis when necessary. The MDIS cameras are mounted on a pivot platform with a rotary drive that provides an operational range of travel of 90° in the YZ plane, 40° from the +Z axis towards the sunshade (-Y), and 50° towards the back of the spacecraft (+Y).

Spacecraft Modes and G&C Activities

From a G&C perspective, flight operations can best be described as the interaction of three spacecraft operational modes with a set of four primary activities. When all systems are performing nominally, the spacecraft is in its “operational” (OP) mode. Demotion to one of two safe modes – safe-hold (SH) or Earth acquisition (EA) - occurs autonomously in response to certain faults or by ground command. Promotion from either of the two safing modes to OP mode can occur only via ground command. The four G&C activities are maintaining spacecraft attitude, managing spacecraft momentum, executing TCMs, and pointing the two solar panels. The system tailors the normal implementation of each of these activities based on the current spacecraft mode. In addition, the G&C system will alter or initiate some activities autonomously in response to certain fault conditions regardless of the spacecraft mode. The interaction of spacecraft modes and G&C activities is summarized in Table 1. More detailed descriptions of each are given in the following paragraphs.

OP mode is the normal mode for science observations and engineering activities. All varieties of the four primary G&C activities can be performed in this mode. Spacecraft attitude is altered by command as needed to point antennas at the Earth, point instruments at various science targets, or align thrusters with a target ΔV direction. A wide variety of pointing options are available for pointing in inertial directions, to various celestial bodies, and to locations on one of these bodies. Scan patterns combining periods of fixed-rate rotations about specified axes with pauses can be added to the base pointing option.⁴

The default spacecraft attitude in the absence of any science or special engineering pointing targets satisfies the dual goals of protecting the spacecraft from the Sun and placing the Earth line in the field-of-view of one of the fanbeam/phased-array antenna sets for communication with Earth. This “downlink” attitude aligns a specified body axis with the Sun line and places the Earth line in one of the quadrants of the XY plane covered by one of the two antenna sets. For most of the mission, the spacecraft will be less than 0.85 AU from the Sun and the Sun direction defaults to the -Y axis so that the sunshade faces the Sun. The +Y axis points at the Sun when spacecraft-Sun range is greater than 0.85 AU, pointing the back of the spacecraft at the Sun. The choice of quadrant for the Earth line depends on the angle between the Sun and Earth directions as seen from the spacecraft and which body axis is being pointed to the Sun. When the Sun-spacecraft-Earth angle is less than 90° and the -Y axis is pointed at the Sun, the Earth vector must lie in the -X,-Y quadrant so that the antenna mounted on the sunshade is used. The back antennas are used when the Sun-spacecraft-Earth angle is greater than 90° since the Earth vector must lie in the +X,+Y quadrant. The opposite antenna sets are chosen when the +Y axis is pointed at the Sun.

Small offsets of the Sun line from the + or -Y axis are allowed to achieve desired observation geometry or to dump momentum passively by altering the solar torque acting on the spacecraft. A fixed offset can be manually commanded, or a variable offset can be computed automatically based on estimated system momentum. The downlink pointing command includes provisions to instruct the software to automatically determine a spacecraft-Sun line offset from the +Y or -Y axis that can achieve a desired target momentum on the X and Z axes while maintaining the spacecraft-Earth line in one of the antenna fields-of-view.⁵ The Y momentum can be adjusted by applying a small change of equal magnitude but opposite direction to each of the solar panels. Attitude offsets from + or -Y to Sun and panel position

adjustments will be used in orbit to minimize the frequency of momentum dumps, which generate small perturbations to the spacecraft trajectory from thruster firings.

Table 1 G&C ACTIVITIES AND SPACECRAFT MODES

Spacecraft Mode	Normal & Autonomous G&C Activities			
	Point & Track S/C Attitude	TCM (ΔV)	Momentum Dump	Point & Track Solar Panels
Earth Acquisition Normal	Sun-relative rotisserie			
Earth Acquisition Autonomous	Sun search as needed		Auto dump as needed (detumble)	Body fixed
Safe Hold Normal	Sun-Earth hold			
Safe Hold Autonomous	Sun-Earth hold modified as needed for hot pole keep-out constraint		Auto dump as needed	Sun track
Operational Normal	Variable targets modified as needed for Sun keep-in or hot pole keep-out constraints	Commanded when needed	Commanded when needed	Sun track Sun track with temperature offset Body fixed
Operational Autonomous	Safing turn (Sun keep-in or hot pole keep-out violation)		Auto dump as needed	

The G&C system enforces two attitude safety constraints in OP mode, both of which arise from the need to protect various spacecraft components from the extreme heat and radiation near Mercury. The first constraint is a Sun keep-in (SKI) zone that is intended to keep the sunshade between the spacecraft bus and the Sun. The Sun line must be kept within specified bounds around the $-Y$ axis in order for the shade to shield the spacecraft components. Although intended to be used when near the Sun, the SKI zone bounds can be defined around any spacecraft body axis. For operational convenience, a SKI zone around the $+Y$ axis is enforced for portions of the mission where Sun range is greater than 0.85 AU. The second constraint is a planet “hot pole” keep-out (HPKO) zone. This constraint keeps the top deck pointing away from the surface of Mercury once the spacecraft is in orbit to protect the battery and other components from radiation reflected off the planet’s surface. The constraint is applied only for certain portions of Mercury’s orbit when it is nearest the Sun and for the portion of the spacecraft orbit when it is nearest the sunlit northern hemisphere. This constraint is not enabled during cruise. When enabled, the G&C system monitors estimated spacecraft attitude for violations of either constraint. If a violation is detected, the system automatically overrides the commanded attitude and performs a turn back to a safe attitude. Demotion to SH mode is requested.

TCMs are executed by command when needed in OP mode, as are momentum dumps to desaturate the reaction wheels. A momentum dump can be combined with any TCM if desired. There are three propulsion system modes corresponding to use of the small, medium, or large thrusters. For a stand-alone

momentum dump or a small ΔV , mode 1 is used to fire a subset of the 4-N thrusters, drawing fuel from the auxiliary tank. For an intermediate ΔV , mode 2 is used to fire the 22-N C thrusters, drawing fuel alternately from the two main fuel tanks. For a large ΔV , mode 3 is used to fire the LVA, drawing fuel and oxidizer from the main tanks. A settling burn using the A1, A2, B1, and B2 4-N thrusters is performed prior to using the main tanks for a mode 2 or 3 burn. For a mode 3 burn, there is also a trim segment where only the C thrusters are firing after the LVA is shut down. The flight software coordinates the operation of the propulsion system components for each of these three sizes of velocity changes. Heater and latch valve configuration is automatically controlled along with thruster firings during the burns. The software also implements a set of initiation and abort checks that insure proper propulsion and guidance system configuration prior to and during thruster firing. The software can abort a burn and request demotion to SH mode if allowable operational ranges are violated.

Solar panel orientation is specified by commanding one of three control modes. There are separate and independent control paths for each panel, although both are commanded to the same orientations for most of the mission. The simplest control mode moves the panel to a specified angle fixed in the body frame; Sun direction is ignored in this mode. The other two control modes orient the panels relative to Sun direction as seen from the spacecraft. The fixed Sun offset mode maintains a constant angle between the Sun line and the normal vector to the panel. The panel rotates as needed to maintain this offset when the spacecraft attitude changes and the Sun direction moves. The third control mode also maintains a desired Sun offset angle but can apply incremental changes to the offset to keep the panel's temperature within a specified range. The fixed Sun offset mode will be used for most of the mission with a zero offset angle (panel face on to the Sun) for most of cruise and offsets ranging between 40° and 60° in Mercury orbit.

The spacecraft enters SH mode when a fault of intermediate criticality is detected. Commanded execution of TCMs or momentum dumps is prohibited in this mode. Spacecraft attitude is restricted to the downlink attitude described above, permitting communication with the Earth via one of the fanbeam antennas. Commands to change to one of the other pointing options are ignored. Offsets from + or -Y axis aligned with the Sun are permitted but will be truncated at the boundary of the SKI zone. If the HPKO constraint is enabled, the attitude will be adjusted away from the downlink attitude when necessary to keep the top deck pointed away from the planet's surface. Once the spacecraft passes out of the defined hot-pole region, normal downlink pointing is automatically reestablished. On entry to SH mode, solar panel control is set to the fixed Sun offset mode using a specially designated value for the size of the offset angle. The offset angle value can be changed or one of the other two control modes can be invoked by ground command once in SH mode.

The spacecraft goes into its lowest level safing mode - EA mode - in response to faults of highest severity. As in SH mode, commanded execution of TCMs or momentum dumps is prohibited, and commands to change to one of the other pointing options are ignored. A specific "Sun-relative rotisserie" attitude is automatically implemented. The rotisserie attitude points a specified spacecraft body axis at the Sun and rotates the spacecraft about this axis at a fixed rate. The nominal EA Sun line is either the +Y or -Y axis, depending on spacecraft range from the Sun, and the rotation rate is 0.0005 rad/s, taking 3.5 hours to complete a single revolution. This rate and the axis can be altered by command. While star tracker data are used if available, the EA attitude can be achieved using only Sun sensor and gyro rate measurements. If both star tracker and Sun sensor data are lost, the system switches to a Sun search routine that performs a series of rotations about each of the body axes until Sun direction information is restored. On entry to EA mode, solar panel control is set to the body-fixed angle mode using a specially designated value for the position angle. The body-fixed angle value can be changed or one of the other two control modes can be invoked by ground command once in EA mode.

In any of the three modes, the G&C system monitors system momentum and will initiate a momentum dump using thrusters when momentum magnitude exceeds limits that could compromise controllability using the wheels. There are two types of autonomous momentum dumps, each triggered by different momentum magnitude levels. The "red" or "leisurely" momentum dump is initiated at a lower momentum level and performs a 1-hour warm up of thrusters by the catbed heaters before firing the

thrusters. The “white” or “immediate” momentum dump is initiated at the higher threshold and fires thrusters with no catbed heater warm-up using a special “cold start” pulsing profile. The system maintains the current attitude using thrusters during the momentum dump and transitions back to wheel control when momentum falls within a specified tolerance of the target magnitude. Only the 4.4-N thrusters are used for commanded or autonomous momentum dumps using propulsion system operational mode 1.

Software Functions and Organization

MESSENGER is equipped with two sets of flight computers, each of which contains one main processor (MP) and one fault protection processor (FPP). The MPs and FPPs are RAD6000 processors operating at 25 MHz and 10 MHz, respectively. A single MP performs all nominal spacecraft functions while the two FPPs monitor spacecraft health and safety. Both the G&C and C&DH (command and data handling) software run in the MP. Only one MP is designated “active” or “primary” and executes the full MP flight software application. The other MP will typically remain unpowered, and does not serve as a “hot spare.” The G&C is implemented in Simulink™ and converted to C code using the RTW™ (Real-Time Workshop) tools, both provided as part of Matlab™. This is integrated with the rest of the flight software, also implemented in C, that operates under the VxWorks 5.3.1 real time operating system.

The G&C software supports the interaction between spacecraft modes and primary activities with the following major functional blocks: attitude estimation, attitude control, guidance, momentum management, propulsion operations, and solar panel control. These functions are split into two main tasks that run at 1 Hz and 50 Hz, respectively. The 50-Hz task contains only those functions necessary for immediate attitude and trajectory control and is streamlined to run as efficiently as possible. Maintaining or changing spacecraft attitude is coordinated by the estimation, guidance, and control functions. The estimation function runs entirely at the 1-Hz rate, and the control functions run at 50 Hz. Guidance functions are split between these two tasks, as are propulsion system operations and momentum management. Solar panel control, phased-array antenna steering, and the MDIS and MLA interfaces run at 1 Hz. The rates, sources, and destinations of data collected from and commands sent to the sensors and actuators are shown in Table 2.

Spacecraft attitude is estimated using an extended Kalman filter algorithm that combines star tracker measurements with gyro rate measurements. Besides the basic attitude and rate, filter states include gyro biases and the relative alignment of the two star trackers. The estimator and attitude propagation algorithms are designed to compute valid estimates when any three or all four of the gyros are providing valid readings. Star tracker rate data are substituted for gyro data if fewer than three valid readings are available. The estimation block also includes “sanity” checks on the sensor data and can reject measurements if they differ too much from preceding values or if they are too noisy. The estimator provides a quaternion correction and gyro biases to the 50-Hz control task used to update its knowledge of spacecraft attitude.

The primary attitude function of the guidance block in the 1-Hz task is to compute the desired (or commanded) spacecraft attitude and rate. Ephemeris models and models for the shape, size, and rotation of a target planet are used when needed to formulate the commanded attitude. Ephemerides stored in the flight processor memory are continuously interpolated to obtain the position and velocity of the Sun, the Earth, a target planet, and the spacecraft referenced to the solar system barycenter. The target planet is either Venus or Mercury, depending on the mission phase. Additional parameters are stored in the flight processor memory for the standard International Astronomical Union (IAU) model giving target planet body-fixed frame orientation relative to the inertial frame and for the triaxial ellipsoid approximation of the planet’s shape and size. Eleven different pointing options are provided and are described in detail in Ref. 4. A simple guidance block in the 50-Hz task propagates the 1-Hz commanded attitude through the intervening 50-Hz intervals between each 1-Hz update.

The 1-Hz guidance block also contains the steering logic for achieving the target ΔV for a TCM. Both fixed inertial vector and time-varying ΔV profiles are supported; the time-varying ΔV is primarily intended for use in the powered turn scenario for MOI. There are three choices for burn termination criteria.

The first is a simple open-loop time option in which the burn is terminated a specified duration after it begins. The second is a closed-loop option in which the burn is terminated when the magnitude of the estimated ΔV is within a specified tolerance of the target magnitude. The third and most accurate option has the same termination criteria as the second option but applies corrections to the commanded quaternion as the burn progresses to better match the desired burn direction. Accumulated ΔV is estimated by the 50-Hz guidance block using a simple low-pass filter applied to the integrated linear velocity readings provided by the accelerometers in the IMU. The current estimated attitude is used to transform the ΔV to the inertial frame.

Table 2 G&C SENSOR AND ACTUATOR INTERFACE RATES

Device	Basic Interface Rate	Measurement or Command	Software Source or Destination	Rate
IMU	100 Hz	Gyro integrated angular rate	1-Hz task	100 samples
		Accelerometer integrated linear velocity Diagnostic data	50-Hz task	2 samples
			50-Hz task	2 samples
			1-Hz task	1 sample
Star trackers (2)	10 Hz	Quaternion and rate rate only diagnostic data	1-Hz task	10 samples
			50-Hz task	latest sample
			1-Hz task	1 sample
Sun sensors (2)	1 Hz	head ID and Sun aspect angles	1-Hz task	1 sample
SADAs (2)	1 Hz	reference and potentiometer voltages	1-Hz task	1 sample
		Step commands	1-Hz task	1 command of up to 100 steps each second as needed
Reaction Wheels (4)	50 Hz	Tachometer time pulse information	50-Hz task	1 sample
		Wheel torque commands	50-Hz task	1 command
Thrusters (17)	50 Hz	On/off commands	50-Hz task	1 command to each thruster as needed when thrusters are firing, but no greater than 1 every second
Latch valves (9), heaters	1 Hz	open/close commands, on/off commands	1-Hz task	1 command to each transponder
Phased-array antennas (2)	1 Hz	Steering commands	1-Hz task	1 command to each transponder
MDIS	1 Hz	Pivot position range and slant angle values	1-Hz task	1 value
MLA	1 Hz		1-Hz task	1 set of values

The attitude control block in the 50-Hz task monitors the difference between actual and desired spacecraft attitude and rate and attempts to drive the error between them to zero by issuing appropriate actuator commands. It provides a choice between two wheel control algorithms and a single thruster control algorithm. MESSENGER is the first mission of the Applied Physics Laboratory (and probably also the first interplanetary mission) to use a nonlinear control law to compute wheel torques.^{6,7} A more traditional time-optimal slew-PID (proportional-integral-derivative) control law is also available as a backup; this is similar to the algorithm used for the Near-Earth Asteroid Rendezvous mission. The nonlinear algorithm has been

chosen as the default for wheel control for reasons discussed in the next paragraph. For either algorithm, when four wheels are available, the controller adds biases to the commanded wheel torques to keep the wheel speeds away from zero; these biases sum to a net zero torque applied to the spacecraft and thus do not alter the control action. These biases are not applied when only three wheels are available, but control is still maintained using the normal logic for the selected algorithm.

With the slew-PID algorithm, a time-optimal slew is achieved by rotating the spacecraft about an eigen-axis with maximum torque until a control switch line is reached. The switch line is then followed by alternating acceleration and deceleration to minimize possible overshoot of the target attitude. Control finally switches to the PID logic once the attitude error falls below a specified small threshold. “Chattering” of the torque values is often seen for some period of time during turns due to the alternating sign of the torque commands when following the switch line. Chattering may add unnecessary stress on the wheel hardware and possibly excite flexible modes if the wheels are capable of following these rapid transitions. The nonlinear algorithm minimizes this chattering of the commanded torques by adjusting their values based on actual attitude error and slew rate, with no explicit sign changes, instead of following a switch line. It is formulated similarly to the PID control logic but has a self-adjusting limiter placed on the proportional and integral attitude error terms. For smaller error values, the computed torques are identical to those of the PID formulation. The nonlinear algorithm can achieve an eigen-axis slew but often deviates slightly from a pure eigen-axis turn, especially when the turn has components along all three body axes. Pre-launch simulations showed no significant difference in total turn time using these two algorithms and elimination of any chattering of the torque commands for most cases using the nonlinear algorithm. The only problem found with the nonlinear algorithm was that the deviation from a pure eigen-axis turn occasionally resulted in SKI violations for turns moving from a point near the zone boundary back towards the center of the zone. The algorithm was modified slightly to limit the size of the deviation from an eigen-axis turn by minimizing the non-eigen axis portion of the slew rate to force the slew axis to remain as close to the eigen axis as possible. The system meets all performance requirements when using this new algorithm, and it produces a more stable torque command profile.

The thruster attitude controller is a standard phase-plane controller. Thrusters are selected to be fired based on the location of switch lines in a phase-plane. A “line of action” is defined for each thruster as the direction of the torque it applies to the spacecraft. The phase plane axes are the dot products of the angle and rate errors with these lines of action. The switch line is chosen such that a thruster is commanded on if it decreases either the angle or rate error. The thruster controller is used during momentum dumps and TCMs and would also be used if fewer than three wheels are available to the controller.

The majority of the propulsion system operation is implemented in the 1-Hz task. This includes all the logic to initiate and terminate a commanded TCM or momentum dump or an autonomous dump, the initiation and abort checks, and configuration of the fuel tanks and heaters while thrusters are firing. Transitions between the various thruster sets for different segments of mode 2 and 3 burns is controlled in the 50-Hz task.

System momentum is computed in the 50-Hz task from the angular speeds of the four reaction wheels and the estimated spacecraft rotation rate. A simple low-pass filter is applied to the estimates to reduce noise on the values. The logic for triggering red or white autonomous momentum dumps also resides in the 50-Hz task.

Fault detection functions are distributed between the 1-Hz and 50-Hz tasks. The 1-Hz task includes the attitude safety constraint monitors that compare the estimated attitude with the boundaries of the active SKI or HPKO zones, health monitoring for the star trackers and IMU, computation of Sun direction from the Sun sensor readings and comparison of this with Sun direction derived from estimated attitude and ephemeris models, and monitors for certain conditions such as aborted TCMs requiring demotion to SH or EA modes. Reaction wheel health monitoring is performed in the 50-Hz task. The G&C software passes various health and status flags and mode demotion requests to the FPPs, which initiate the appropriate response, if any.

The primary MP interfaces to two Data Processing Units (DPUs) and the two FPPs via the 1553 data bus. The DPUs provide the interface to all other instrument processors. G&C software in the MP passes data to the primary DPU to route attitude data to the imager and laser altimeter instruments, and to actively steer the imager pivot motor.

DETUMBLE

The first test of the G&C system was establishing attitude control by detumbling after separation from the launch vehicle. Detumble was performed as a tailored form of the autonomous red or leisurely momentum dump. Catbed heaters were turned on before launch so that the thrusters would be warm enough to fire after separation if needed. Timing and momentum thresholds were altered to ensure that the red dump configuration would be executed if the tip-off rate exceeded the control authority of the reaction wheels. A & B (4.4 N) thrusters fired for around 50 s between MET (Mission Elapsed Time)* 5315 and 5365 to null the tip-off rate of 0.03 rad/s (1.72°/s, 0.29 rpm). Control then transferred to the reaction wheels, turning the spacecraft to point the +Y axis at the Sun by MET 5450. Solar arrays were rotated 180° from their deployed position to place the cell side toward the Sun by MET 5520. Figure 5 shows the body rates as propagated in the 50-Hz control task from gyro data from the time of IMU turn on until shortly after control transferred to the wheels.

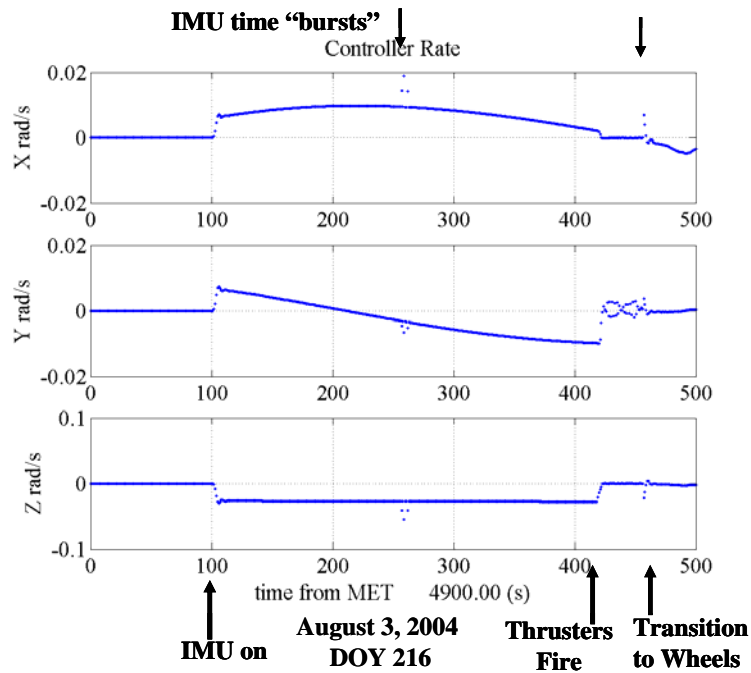


Figure 5 Detumble Rotation Rates

Thruster fuel lines were evacuated (“burped”) and fuel was allowed to “bleed in” to the lines prior to detumble. The “bleed in” activity sent commands to open the auxiliary tank bleed valve (AFTLV1) and also performed a sequence of rapid open/close commands to “flutter” the main auxiliary tank valve (AFTLV2). Thruster firings during detumble drew fuel from the auxiliary tank via AFTLV1 instead of AFTLV2. Propulsion preparation and clean up for the detumble momentum dump only operated heaters and did not manipulate latch valves. This was an alternate path for executing the autonomous dump; normally AFTLV2 would have been commanded open and then closed in the preparation and clean-up.

* MET was set to 1000 at the time of launch August 3, 2004 06:16 UTC; it increases at roughly 1 s/s, so that any given MET is approximately 1000 s greater than the time since launch in seconds.

This path was selected because of an artificial detection of an “over current” condition when AFTLV2 was “fluttered”. Subsequent testing has shown no problems with latch valve operation and the “over current” condition has not recurred, including during TCM operations.

Thrusters were pulsed more often than expected in the “coasting” period after the initial rate was nulled and before control transitioned to reaction wheels. Approximately 230 g of fuel were used, which is probably more than should have been needed. This was traced to an incorrect sign on the values of some of the phased-plane controller parameters. The values loaded to the spacecraft for detumble were checked many times by the G&C team and were the intended values. Unfortunately, the sign error was missed in these checks. All of the simulations using these values resulted in successful detumbles; high-rate thruster firing histories were not examined in detail due to schedule constraints. As the values were not grossly wrong in that they did not lead to any instability or inability to detumble, detailed checks were not made. These values were specially selected for the detumble conditions and were replaced with the normal values at first contact (about 6 hours after launch). There is no sign problem for these default values (as confirmed by performance during TCMs 1, 2, and 3).

Star tracker 1 was turned on after detumble around MET 5630. It produced one valid attitude solution and then failed to maintain lock and reverted to its standby mode. Diagnostic data indicate that only two stars were visible to the tracer, where at least three are needed for a valid attitude solution. A reset by autonomy action failed to correct this. Two hours later, star tracker 1 was powered off, and star tracker 2 was turned on and remained in its normal tracking mode. Analysis of the initial spacecraft attitude history has shown that there were no bright bodies (Sun, Earth, Moon) near the field-of-view of the trackers at turn-on time. The remaining possibilities are that something was floating through the field-of-view to obscure the star images (a fuel cloud from detumble thruster firings, part of the third stage, or other material outgassing from the spacecraft) or glint from some part of the spacecraft or a nearby object that later moved away from the spacecraft.

All six Sun sensor heads detected the Sun at various times before thrusters were fired for detumble; since then only heads 5 and 6 have been pointing at the Sun as they are on the +Y side of the spacecraft.

EARTH ACQUISITION MODE ATTITUDE CONTROL

After detumble, the spacecraft continued in the normal EA mode attitude, pointing the +Y axis at the Sun with a commanded rotation rate of 0.0005 rad/s about the +Y axis, until August 9. During the first few days, it was noticed that the actual rotation rate was slowly decreasing. The rate computed by the attitude estimator stayed relatively constant at the expected value, but the rate derived from differencing the estimated attitude quaternions was slowly decreasing, as shown in Figure 6. At the same time, the estimated gyro biases were continually increasing. These gyro biases are passed to the control algorithm and used in its processing of the gyro readings. The erroneous gyro biases caused the controller to compute a rate close to the commanded rate, so no changes were made to the wheel torques to counter the actual decrease in rate. The estimator was reconfigured to stop estimating gyro biases on August 6, and the rotation rate returned to the commanded value. Gyro biases were not estimated again in EA mode except for a brief period just prior to promotion to OP mode on August 9. On that day, the estimator was reset and configured to estimate gyro biases for a few hours then reset again and configured not to estimate gyro biases. Detailed telemetry data were collected during this period to aid in the analysis of the estimator’s behavior. The data showed that the gyro bias estimate on the Y axis again erroneously increased after the estimator was reset when the filter was configured to estimate the biases.

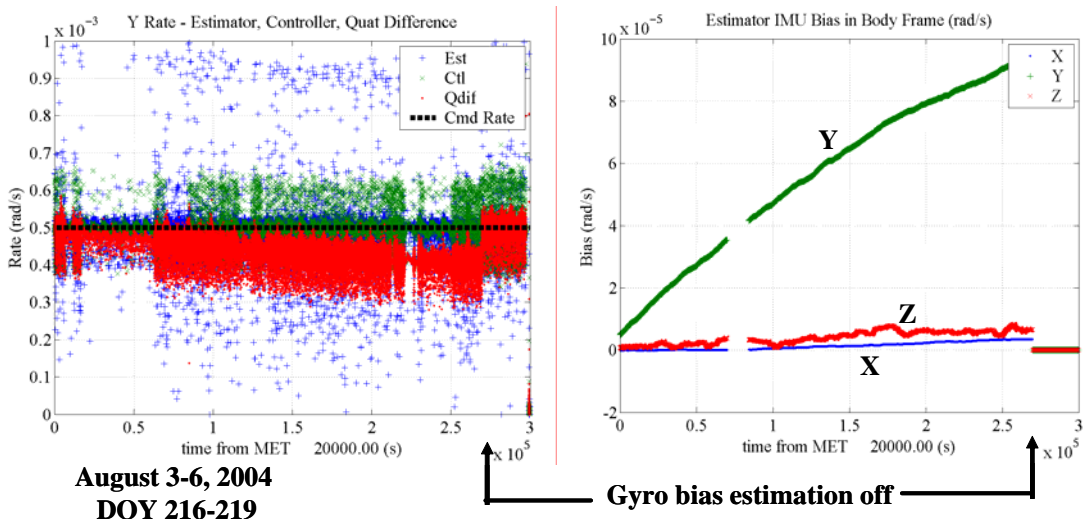


Figure 6 Estimated Rate and Gyro Biases in EA Mode August 3-6, 2004

Further investigation has traced the EA mode behavior to the estimator’s response to the pattern of time tags and validity flags for the IMU gyro data produced by drift between the IMU’s internal clock and the MP clock. This clock drift was known before launch, but this long-term effect on the EA mode attitude was not anticipated or seen in the few-hour ground tests of EA mode where the real IMU was used. The actual time tag pattern seen in flight (and in ground tests) has “bursts” of irregularly spaced measurements that recur approximately every 200 s as shown in Figure 7. These include repeated measurements where the actual time change between measurements is 0, skips in the measurements where the actual time change is 0.02 s, and irregular jumps where the time change is somewhat less than or greater than 0.01 s.

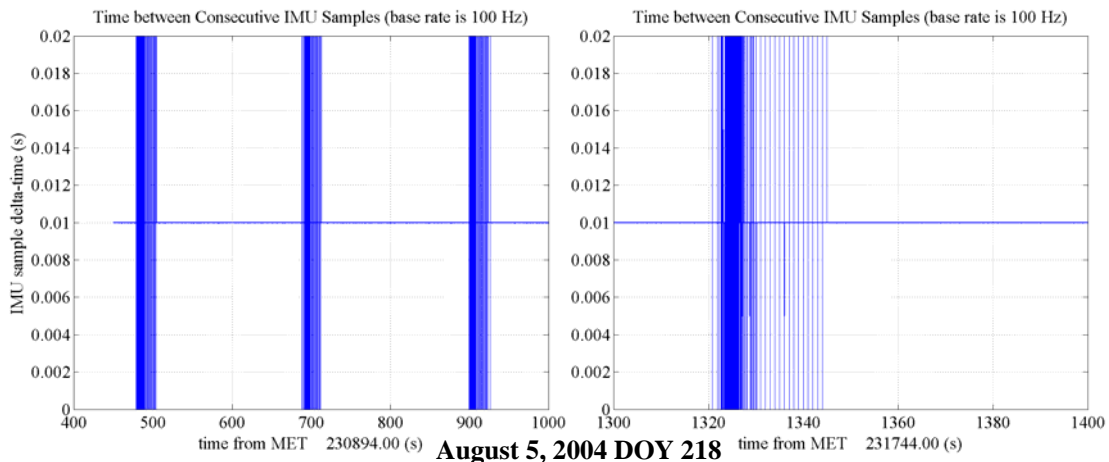


Figure 7 IMU Time Tag Drift Pattern (from flight telemetry)

The code that reads the 100-Hz messages from the IMU and formats the data for input to the 1-Hz and 50-Hz G&C tasks was designed for a much smaller clock drift rate and made certain assumptions that would be valid for a near-perfect synchronization between the two clocks. Instead of passing the actual time tags generated by the IMU to the G&C tasks, this interface software generates an artificial regular pattern of time tags differing by 0.01 s between each consecutive measurement. It examines the time tags for the IMU samples and applies one of the regularly-spaced times unless a sample is identical to the one immediately preceding it. In the case of a repeated measurement, the software sets the time tag for the second measurement to 0 and marks it as invalid. The resulting time tag sequence is the time tag pattern expected for an exact match between the IMU and MP clocks with the exception of the repeated

measurements. A typical time tag sequence for perfectly matched clocks would be 100.01, 100.02, 100.03 s; the same sequence with repeated measurements, skips, and irregular jumps might be 100.01, 100.01, 100.03, 100.05, 100.061, 100.07, 100.079, 100.09, etc. The current software would produce a sequence of 100.01, 0, 100.03, 100.04, 100.05, 100.07, 100.08, 100.09. The integrated angular rate and linear velocity counts for each sample are passed on unchanged from the IMU with these time tags.

The estimator checks the time change between consecutive measurements as well as the validity flags. It rejects gyro measurements if the time change between two samples is less than zero or greater than a certain threshold and also rejects measurements flagged as invalid on input. It substitutes rate measurements from the star trackers, which are inherently noisier than the gyro readings, when the gyro measurements are rejected. When a repeated IMU sample occurs, the estimator must transition from gyro to tracker rate and back again for three or four of the 0.01-s time steps in its rate propagation. This frequent switching between rate sources and the attendant filter reconfiguration caused the estimator to attribute actual rotation about the Y axis in EA mode to a gyro bias. There is never a long enough period of time with a regular pattern of IMU data for the filter to correct this error. The high amount of rejected IMU gyro samples during the “burst” periods also causes the estimator to periodically report a drop in the quality of the attitude estimate.

While repeated IMU samples seem to have the largest effect on the estimator, the skipped samples have a potentially more serious effect on the performance of the 50-Hz controller tasks. Angular rate and translational acceleration are propagated in this task using two consecutive samples of gyro and accelerometer measurements. No time tags are passed in and the time change between the samples is assumed to be 0.01 s. For a repeated measurement, one of the two samples is invalid and the software ignores both new samples and uses its last value for rate or acceleration. When the gyro or accelerometer counts reflect the rate or velocity change over a time period different from 0.01 s, the software computes the wrong rate or acceleration due to the erroneous assumption for the time increment between the two samples. The worst case occurs for a skipped measurement where the time change between the two samples is 0.02 s. The resulting “hiccups” or small, temporary jumps in estimated rate do not seem to be causing a noticeable response by the controller so far, but they may cause problems in meeting the pointing accuracy and stability requirements for precise science observations. The corresponding hiccups in estimated body acceleration during thruster firing can affect TCM performance if the burn is terminated prematurely due to the “extra” ΔV that seems to accumulate over any intervals with skipped samples. This possibility led to the decision to alter the target ΔV for TCM 1 as discussed in a later section. (An example of a rate “hiccup” is shown in Figure 5 from detumble, while Figure 8 includes one for estimated body acceleration that occurred during TCM 1.)

Prior to launch, the G&C team had identified the need to add a model for this IMU time drift to its ground stand-alone simulations. It was known that this caused periodic drop-outs of some percentage of the IMU data samples that should be included in simulations for future events. This model was implemented shortly after launch to aid in the analysis of the effects seen in the first few days of EA mode. The results of this more extensive analysis have also led to a decision to proceed with a new flight software build to better handle the actual data pattern as read from the IMU. The IMU data interface is being altered to provide time tags as generated by the IMU to both G&C software tasks. This change should eliminate the “hiccups” in estimated rate or acceleration as the time increment between consecutive samples will match the rate and velocity counts. The estimator logic for transitioning between gyros and star tracker as a source of rate is being altered to switch to tracker rate only when there is a long-term outage in the gyro data. Both the estimator and controller will retain memory of a longer sequence of IMU data samples and will use values from the last valid samples for some time before switching over to another source of rate information. Star tracker rate will no longer be substituted for gyro rates when running the Kalman filter. Instead, the estimator will simply report star tracker estimated attitude and rate directly when it switches to the tracker-only mode. Many of these changes have already been incorporated in the G&C software for the New Horizons mission, but they were recommended too late in the development cycle to be incorporated in the MESSENGER software prior to launch.

G&C SYSTEM TESTING

A series of in-flight tests were defined prior to launch to check out (or commission) the G&C hardware components and software functions. The tests were divided into two sets, an immediate check-out of the simpler functions and hardware that could be performed while in EA mode and a more extensive set checking the higher-level functions to be performed once the spacecraft was promoted to OP mode. The EA mode tests were performed on August 6, 2004. The first test simply collected Sun direction readings from each of the three Sun sensor heads and exercised the commands to change sensitivity threshold for the two DSS systems. As expected, only the two heads on the back of the spacecraft reported valid Sun presence. This test will be repeated in April 2005 after the spacecraft is “flipped” to have the sunshade (-Y axis) pointing at the Sun, at which time all four heads mounted on the shade should report valid Sun presence. The second test exercised processing of quaternions from each of the two star trackers by the attitude estimator and also the ability to vary the EA rotation rate in both direction and magnitude from the default value. Both star trackers performed nominally during this test, but a software error was discovered that erroneously reported a hardware problem with one tracker when it was powered on but not selected for use by the estimator. (This error is being corrected as part of the new flight software build.) Rate changed as expected in response to parameter loads to alter the desired rate; rates of a few tens of $\mu\text{rad/s}$ were successfully achieved, demonstrating a capability being used for instrument calibrations.

The tests performed after promotion to OP mode covered the SADA functions and solar panel control modes, the two wheel control algorithms, and IMU functions and calibration. The test of solar panel control was performed on August 11 and exercised the body-fixed and fixed Sun offset control modes. The panels were manually commanded to positions at 265° and 275° using the body-fixed control mode; these positions were each 5° away from the nominal 270° position representing face-on to the Sun at the default downlink attitude. For the fixed Sun offset mode, panel motion was induced both by changing the desired Sun offset angle from 0 to 5° and by altering the nominal downlink attitude to point an axis offset 5° from the -Y axis at the Sun. In the first case, the panels moved away from the face-on to Sun position in response to the new offset angle. In the latter case, the Sun offset angle remained at 0 and the panels moved in response to the attitude change to maintain their face-on to Sun orientation. This 5° “tilt” away from -Y to Sun was the first change from the default downlink attitude in OP mode and the first demonstration that the Earth line could successfully be maintained in an antenna quadrant with the -Y axis offset from the Sun line.

The wheel control test performed on September 9 consisted of a series of rotations at $0.15^\circ/\text{s}$ in both directions about the Y, X, and Z body axes. The rotation sequence was performed twice with all four wheels being used for control, once using the non-linear control algorithm and again using the slew-PID algorithm. The sequence was then repeated four additional times using the non-linear algorithm, each time with one of the four wheels removed from the control loop (while still powered on). This test verified the correct implementation of both control algorithms and the ability to switch to the slew-PID algorithm as a backup to the non-linear algorithm. The ability to maintain control if spacecraft autonomy removes one of the reaction wheels from the control loop was also confirmed.

The final G&C test was designed to verify IMU hardware functionality and acquire data to be used in ground estimation of IMU calibration parameters such as gyro alignment and scale factor errors. The need for in-flight calibration was identified prior to launch due to problems with vendor calibration and the possibility of gyro alignment shifts that could result if inadequate welds in the gyro housing failed. Hardware functions were tested by configuring the IMU to operate from each processor board with all four gyros and accelerometers active and also with only the four gyros active. A series of rotations about the X, Y, and Z body axes at a rate just under $0.3^\circ/\text{s}$ was executed while collecting gyro and star tracker data for the calibration solutions.⁸ Data were collected while rotating with the IMU operating from each of the processor boards, as the calibration is known to be different between the two. The rotations were also repeated while the estimator was configured to use each star tracker alone and to use both. The first attempt

to perform this test on September 13 was aborted prematurely by an unexpected demotion to SH mode that was unrelated to any G&C activity. It was rescheduled and successfully ran to completion on October 6. This test will be repeated approximately every 6 months throughout cruise, and calibration parameters will be updated as needed should the ground solutions indicate significant changes as the IMU ages.

No explicit tests are planned for the remaining G&C functions such as pointing options that target locations on a celestial body, steering of the phased-array antenna, or operation of the propulsion system. Instead, these functions are being tested by conducting normal spacecraft operations. The back phased-array antenna has been in use since September 2 with boresight direction information being provided by the G&C software. The front phased-array antenna will be checked in February and March of 2005 when the Sun-spacecraft-Earth angle becomes greater than 90°. The propulsion system has been operated for detumble in mode 1 and in mode 2 for the first 3 TCMs as discussed below. Operation in mode 3 with first use of the LVA main engine will occur for DSM 1 in December 2005. Additional pointing options, in combination with scan patterns, will be exercised with the various science instrument observations of the Earth and Moon running from May 2005 through the Earth flyby in August 2005.

SAFE-HOLD AND OPERATIONAL MODE ATTITUDE CONTROL

The spacecraft was commanded to operational mode on August 9, 2004. This was the first test of the true 3-axis inertial attitude mode for the G&C system. The transition to the downlink attitude went smoothly. The time of the mode change was chosen such that only a very small turn was needed to null the EA rotation rate and put the Earth line in the back antenna (+X,+Y) quadrant. Gyro bias estimation by the Kalman filter was turned on for several hours just after promotion to OP mode, and the behavior described above for EA mode did not recur. This had been predicted since the commanded rate is usually zero for operational mode attitudes. Gyro bias estimation has remained off since then, despite the results of this test, as it is not absolutely necessary to meet current pointing accuracy requirements. The majority of the time since entering OP mode has been spent at the default downlink attitude with the +Y axis pointing at the Sun. The non-linear wheel control mode has been in use except for a portion of the wheel control test on September 9 and while thrusters were firing for TCMs 1, 2, and 3.

An intentional demotion to SH mode and promotion back to OP mode was performed on August 10, primarily to test autonomy response and recovery procedures. There was no change in attitude control as the default SH mode attitude is identical to the default downlink attitude in OP mode. The unplanned transition to the SH attitude that occurred during the first attempt at the IMU calibration did require a turn back to the downlink attitude as the spacecraft had rotated away from it following the scan pattern designed for that test. The turn and stabilization at the SH downlink attitude proceeded without incident. Both of these SH periods exercised the different logic paths in the guidance software that compute the default downlink attitude in SH mode versus OP mode.

Attitude changes performed in OP mode to date were done either as part of G&C system tests or for some engineering or science activity. An offset was applied to the default +Y-to-Sun downlink attitude for the solar panel control test on August 11 and again to allow the MDIS radiometric calibration target to be illuminated by the Sun on November 29, 2004, and January 12, 2005. The offset was as only 5° for the solar panel control test, but was 27° for the MDIS calibration target viewing, placing the Sun at elevations of +5° and -27° but retaining the 0° azimuth. Solar panel motion had to be restricted for the MDIS test as the normal face-on to Sun orientation would have moved to a position beyond the hardware stops of the SADAs. The spacecraft was turned to point the +Z axis (nominal C thrust direction) in the target ΔV direction for TCM 1 on August 24, for TCM 2 on October 24, and for TCM 3 on November 18; a “practice” version of TCM 1 was performed on August 18 that included the turns to and from burn attitude but no thruster firing. For all three TCMs, the attitude had only a small offset of the -Y axis from the Sun line (Sun elevations of 3.24°, 2.77°, and -1.41° respectively) with a large rotation of the Earth line well out of the XY plane away from either antenna quadrant. The special burn pointing option was used for the turns to burn attitudes with the downlink pointing option being commanded for the turn back. One of the more complicated attitude changes performed to date was a scan that moved the +Z axis around the location of

the star α Leo (Regulus) so that it could be observed by the MASCS instrument. The date of this observation, December 8, 2004, was chosen such that the Sun-spacecraft-star angle was nearly 90° and the turn to the initial attitude was mostly a rotation about the Y axis. The scan pattern covered a region of 2° about the X and Y body axes, centered on the star location. The rotation rate was set to $70 \mu\text{rad/s}$ to allow the star to move slowly through the instrument field-of-view. Initial results show that the star was sensed very near the center of the scan pattern indicating good pointing control as well as alignment of the MASCS boresight relative to the +Z axis. A similar star observation, without a scan pattern, is scheduled for February 7-9, 2005, as part of the XRS instrument check out. Both of these use the “+Z” pointing option which accepts a target for the +Z axis as the primary boresight while maintaining the Sun as close as possible to the +Y axis (or -Y axis for outer cruise).

TCMs 1, 2, and 3

The first TCM of the mission was scheduled for August 24, 2004, and was intended to correct launch injection errors. The original target for this TCM based on navigation solutions called for a ΔV magnitude of $\sim 21 \text{ m/sec}$. The burn was to be executed using the C or 22-N thrusters using propulsion mode 2, as it was not desired to operate the LVA so early in the mission. The total burn duration at this magnitude would be 256 s. During the first weeks of flight while TCM 1 was being designed, the G&C team was investigating the effects of the IMU time drift. As previously mentioned, one of the potential effects was an incorrect computation of accumulated ΔV over a skipped accelerometer measurement. Since the IMU time “bursts” are spaced roughly 200 s apart, there was concern over performing a burn long enough to include more than one of these episodes. Prior to launch the propulsion team had predicted significant impingement for the C thrusters. The G&C software had been modified to accommodate this, but TCM 1 would be the first time the thrusters were fired in flight and the effects of impingement possibly observed. For these reasons, it was decided upon recommendation by the G&C team to reduce the magnitude of TCM 1 to exactly 18 m/s along the same target direction as the original design. This would make the burn duration close to 200 s insuring that if a time burst did occur while thrusters were firing it would only be once. The mission design and navigation teams confirmed that making up the remaining ΔV at subsequent TCMs did not adversely affect the ΔV budget for the mission. The next two TCMs were rescheduled for October 24 and November 18, 2004 (previously TCM 2 would have been in November; the new TCM 2 on October 24 was added as the second segment of the original TCM 1.) TCM 1 execution was nominal, and it provided much useful data on C thruster performance. The on-board estimated body acceleration and inertial ΔV are plotted in Figure 8. There was one IMU time burst during the burn as can be seen in the plot of the Z acceleration component (C thrusters generate ΔV in the +Z direction).

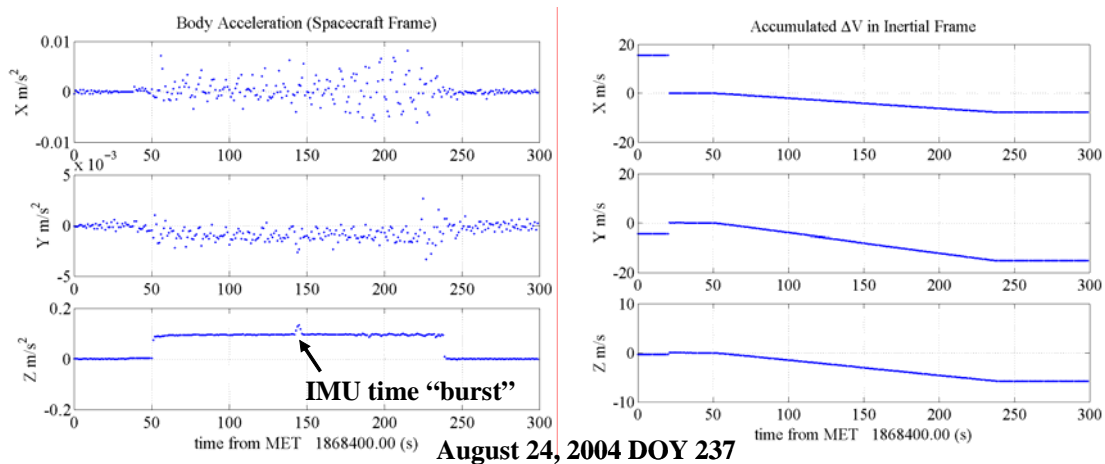


Figure 8 Acceleration and Accumulated ΔV for TCM 1

TCMs 2 and 3 were performed as scheduled, with target ΔV magnitudes of 4.6 and 3.2 m/s, respectively. Both of these TCMs also used the C thrusters for the main burn. All three TCMs have used propulsion mode 2 which begins with a 15-s settling burn where the A1,A2 and B1,B2 thrusters are fired continuously. The settling burn was followed by a main burn segment where all four C thrusters were pulsed as needed to achieve the target ΔV given the possible effects of impingement. The duty cycle for the C thrusters was 99.7% for TCM 1 (C1,C2,C3, and C4 pulsed), 100% (continuous firing) for TCM 2, and 99.96% (only C1 pulsed) for TCM 3. The main burn was terminated when the target ΔV was reached, with the 4.4-N thrusters continuing to be used for attitude control for an additional 30 s while the propulsion system was placed back in its idle configuration. The total duration of thruster firing for TCM 1, 2, and 3 was 231.56, 88.86, and 63.86 seconds, respectively. There were no IMU time bursts during thruster firing for TCMs 2 and 3, which is not surprising given their much shorter duration compared to TCM 1. The propulsion team recommended a strategy for fuel tank usage that would move the spacecraft center-of-mass closer to alignment for the C thrusters and then back to alignment with the LVA over the TCMs leading up to DSM 1. TCM 1 used main fuel tank 1, while TCMs 2 and 3 have used fuel tank 2. Operation of all latch valves, heaters, and thrusters has been nominal. Propellant usage for the 3 TCMs was 8.88 kg, 2.35 kg, and 1.7 kg, respectively.

Table 3 shows the execution accuracy for TCMs 1, 2, and 3. It compares the target ΔV with the on-board estimate and with reconstructions provided by the navigation team and by the G&C team. The navigation solution is based on Doppler and range tracking data taken during and after each burn and is the more accurate value; these are considered the official achieved ΔV s for each TCM. The G&C reconstruction is based on ground processing of high-rate IMU accelerometer data to re-estimate the imparted ΔV . Any “hiccups” due to the IMU time drift are removed in these ground solutions. The on-board estimate is taken directly from flight telemetry at the time of the last thruster firing. The table presents magnitude and pointing errors for each TCM. The magnitude error is the difference between the reconstructed and target ΔV magnitude given as a percentage of the target ΔV magnitude. The pointing error is the angle between the reconstructed ΔV direction and the target ΔV direction. The smaller TCMs 2 and 3 have somewhat larger execution errors, but this was predicted by ground simulations prior to launch and performance is actually somewhat better than anticipated. Note the difference between the on-board and ground G&C magnitude errors for TCM 1. This is due to removing the effect of the “hiccup” in estimated acceleration from the IMU time burst shown in Figure 8.

MOMENTUM MANAGEMENT

In the first month after launch, the system momentum was increasing at a greater rate than had been expected from pre-launch simulations. In particular, the Y momentum was growing at the fastest rate. This is believed to be due to solar pressure acting on the irregular surface of the back of the spacecraft that is currently pointed at the Sun. The model for this side of the spacecraft was not expected to be as accurate as the one for the regular surfaces of the sunshade pointing at the Sun. The momentum had reached high enough levels just prior to TCM 2 that it was decided to add a momentum dump to the TCM. While this changed the momentum value, the steady build-up on the Y axis remained after the TCM. The G&C team proposed using the solar panels to generate a torque on the Y axis to counter this build up. This had always been part of the planned passive momentum dumping in Mercury orbit, but in this case the offset in panel angles was applied manually since the solar torque model was not considered accurate enough to permit computing the angle on-board using momentum feedback. An experiment was performed on September 27 where the panels were moved to positions that differed by 30°. The momentum changes observed during this test, combined with similar data from the previous weeks of flight, were used to compute an offset that would lower the Y axis momentum to near zero. This offset of only 2.7° was applied starting on October 8 and has been in effect for all periods at the downlink attitude since then, successfully decreasing the Y momentum change to a tolerable level. Although the momentum was not particularly high prior to TCM 3, it was decided to add a momentum dump to this TCM as well. This was done to insure that the momentum would remain well below the threshold for an autonomous dump until late March 2005 when the spacecraft will be turned to point the shade at the Sun. The target momentum value for the dump with TCM 3 was chosen based on extrapolations of momentum change seen in flight up to TCM 3. Momentum has been

closely following this prediction since TCM 3 was executed, achieving the lowest values yet seen in flight in December 2004. Momentum magnitude has begun to increase again in the first months of 2005. Momentum change will be carefully monitored after the upcoming change to point the sunshade at the Sun, as this will be the first opportunity to compare the shade solar torque model with in-flight data.

Table 3 EXECUTION ACCURACIES FOR TCMS 1, 2, AND 3

	ΔV Vector in EME2000 Inertial Frame				Proportional Magnitude Error	Pointing Error
	X	Y	Z	magnitude		
	(m/s)	(m/s)	(m/s)	(m/s)	(%)	(°)
TCM 1						
Target	-7.7884	-15.1734	-5.7539	18		
NAV reconstruction	-7.8279	-15.0637	-5.6788	17.9009	-0.508	0.31
On-board estimate	-7.8147	-15.2208	-5.77	18.056	0.31	0.009
G&C reconstruction	-7.771	-15.105	-5.736	17.929	-0.39	0.053
TCM 2						
Target	0.1004	-4.1813	-1.8906	4.5899		
NAV reconstruction	0.08617	-4.1872	-1.8749	4.5885	-0.03	0.274
On-board estimate	0.1076	-4.1949	-1.895	4.6043	0.31	0.089
G&C reconstruction	0.1093	-4.1955	-1.8934	4.6043	0.31	0.11
TCM 3						
Target	2.2463	-2.1654	-0.8603	3.2365		
NAV reconstruction	2.2448	-2.18609	-0.85246	3.24727	0.333	0.322
On-board estimate	2.26232	-2.1744	-0.8504	3.2510	0.45	0.263
G&C reconstruction	2.2612	-2.1764	-0.8519	3.252	0.48	0.23

CONCLUSION

Overall, the MESSENGER G&C system has been performing well since launch in August 2004. The spacecraft has responded correctly to commanded attitude and rate changes and the desired attitudes have been maintained within the accuracy needed for current flight operations. Momentum build-up in the first few months of the mission was higher than anticipated. This is probably due to a poor model of the back side of the spacecraft that is currently being exposed to the Sun. Solar torque generated by tilting the solar panels at slightly different angles has been used to passively counter this build up. The observed inability to maintain the desired rotation rate in EA mode has led to a fuller understanding of the impacts of the time drift between IMU and MP clocks given the existing flight software design. A few of these impacts have been judged serious enough to warrant implementation of new flight software to accommodate the actual timing pattern. The new software is scheduled to be uploaded to the spacecraft and

tested in-flight in fall of 2005. This should eliminate any problems with accelerometer data processing for the first DSM using the LVA in December 2005 and all other future TCMs. This should also allow the system to meet its performance requirements for science observations to be performed at the Earth, Venus, and Mercury flybys and in Mercury orbit.

ACKNOWLEDGEMENT

The work described in this paper was performed at The Johns Hopkins University Applied Physics Laboratory, under contract (NAS5-97271) with the National Aeronautics and Space Administration, Discovery Program Office.

REFERENCES

1. S. C. Solomon et. al., "The MESSENGER Mission to Mercury: Scientific Objectives and Implementation," *Planetary and Space Science*, Vol 46, Issues 14-15, pp. 1445-1465, December 2001.
2. A. G. Santo et. al., "The MESSENGER Mission to Mercury: Spacecraft and Mission Design," *Planetary and Space Science*, Vol 46, Issues 14-15, pp. 1481-1500, December 2001.
3. R. E. Gold et. al., "The MESSENGER Mission to Mercury: Scientific Payload," *Planetary and Space Science*, Vol 46, Issues 14-15, pp 1467-1479, December 2001.
4. D. J. O'Shaughnessy and R. M. Vaughan, "MESSENGER Spacecraft Pointing Options," AAS/AIAA Spaceflight Mechanics Conference, AAS-03-149, San Juan, Puerto Rico, Feb. , 2003.
5. R. M. Vaughan et. al., "Momentum Management for the MESSENGER Mission," Paper AAS 01-380, AAS/AIAA Astrodynamics Specialists Conference, Quebec City, Quebec, Canada, July 30-August 2, 2001.
6. B. Wie, D. Bailey, and C. Heiberg, "Rapid Multitarget Acquisition and Pointing Control of Agile Spacecraft," *Journal of Guidance, Control, and Dynamics*, Vol. 25, No.1, Jan-Feb 2002, pp. 96-104.
7. Shapiro, H. S., "Implementation of a Non-linear Feedback Control Algorithm for Large Angle Slew, and Simulations from MESSENGER Applications," APL internal memo SRM-02-032, May 12, 2003.
8. Pittelkau, M. E., "Attitude Determination and Calibration with Redundant Inertial Measurements Units," AAS/AIAA Space Flight Mechanics Conference, AAS 04-116, Maui, HI, February 8-12, 2004.